NGI Technical note

To:	Norges vassdrags- og energidirektorat (NVE)
Attn.:	Aart Verhage
Copy to:	Odd Are Jensen
Date:	2020-06-26
Revision no./Rev.date:	0 /
Document no.:	20170131-19-TN
Project:	SP4 FoU Snøskred
Project manager:	Dieter Issler
Prepared by:	Kjersti Gisnås
Reviewed by:	Christian Jaedicke

Wind simulations for use in local avalanche forecasting

Contents

Appendix

Review and reference page

NORWEGIAN GEOTECHNICAL INSTITUTE
NGI.NO

Main office
PO Box 3930 Ullevaal St.
NO-0806 Oslo
Norway

Trondheim office
PO Box 5687 Torgarden
NO-7485 Trondheim
Norway

T 22 02 30 00
F 22 23 04 48
NGI@ngi.no

BIC NO. DNBANOKK
IBAN NO26 5096 05 01281
ORGANISATION NO.
958 254 318MVA

ISO 9001/14001
CERTIFIED BY BSI
FS 32989/EMS 612006

1 Introduction

Quantification of release probabilities in local avalanche forecasting are depending on knowledge of historical weather characteristics as well as detailed knowledge of the wind driven snow distribution on a fine scale. In WP5 we have computed extreme weather statistics for snow and other related parameters for historical and future climates at 1 km^2 resolution (2), and prepared gridded regional scale wind data for use in statistics together with historical gridded data (3). Within each 1x1 km grid cell wind is the dominant factor determining snow distribution in the terrain. Simple terrain indexes as well as a complex fluid dynamic (CFD) model have been tested and evaluated with respect to performance in modelling wind fields (4), determine snow distribution (4.7) and potential release areas (4.8). Several scripts and tools have been developed along this study with the aim of establishing an improved toolbox for avalanche forecasting on a local scale.

2 Access and analysis of gridded climate data

2.1 Historic and prediction data for temperature, precipitation and snow

Extended use of homogenized gridded historical weather data from Senorge (www.xgeo.no) has been explored for understanding snow cover characteristics and related weather parameters (Appendix, Figure 19). To also understand the potential future changes in winter climate, prediction data from the Norwegian Centre for Climate Services (NCCS) has been included. For selected climate models and emission scenario (rcp 4.5 or 8.5), relative changes from reference period to the end of the century are analysed for monthly precipitation, temperature and snow cover (example from Finse in Appendix, Figure 20, IPSL and rcp8.5) as well as annual precipitation, maximum snow water equivalent and snow covered days (Appendix, Figure 21 and Figure 22).

The effect of climate changes on the avalanche danger is complex. The number of snow-covered days will be reduced in most regions, resulting in lowered probability for avalanche situations. On the other hand, extreme snow fall events will increase in intensity in many regions, and in some also in frequency. Winter air temperatures increase over all of Norway, resulting in less frequent long cold periods and more frequent temperature fluctuation close to 0° C in many regions prone to avalanches. Warmer temperatures are favourable for stabilization of the snow pack, and thus this effect will contribute to reduced avalanche situation frequency. Snow cover in the lower parts of steep maritime avalanche paths in western Norway will be more unusual, which may contribute to increased friction and reduced run-out distances. These changes, particularly in areas with increasing avalanche risk, should be accounted for. Development of such methodologies are ongoing at NGI.

Timeseries of wind data are not included in the historical SeNorge dataset and are also currently not available from the Klima2100 report. It is therefore difficult to quantify how this will change in the future. However, with wilder climate it is likely that the frequency and intensity of strong winter storms will increase in the future.

2.2 Modelled wind data

There is currently no operational gridded dataset for wind data with long continuous data series available that represents "over land" wind directions and speeds sufficiently well to be used in local avalanche forecasting. However, dataseries of daily averaged data from AROME for the period September 2016 to 2019 have been made available from MET/NVE. These are downscaled to the same grid and temporal resolution as the SeNorge dataset, and wind speed and directions aggregated over 24 hours for 06-06 UTC. Wind directions are averaged to 8 main directions using Labert's formula. The dataset has proven to reproduce observed wind speed and directions at Finsevatn and Kvitenova well (Figure 1and Figure 2). The dataset is coarse both in temporal and spatial resolution but is suitable for generation of wind statistics in combination with SeNorge air temperature, precipitation and snow fall data for any point location in Norway. A MATLAB tool has been produced to easily generate wind roses for a given coordinate, with the option to analyse wind distribution when the snow height is > x cm, and for days with precipitation as snow > x. The tool is also prepared for exporting timeseries of wind data to WindSim format.

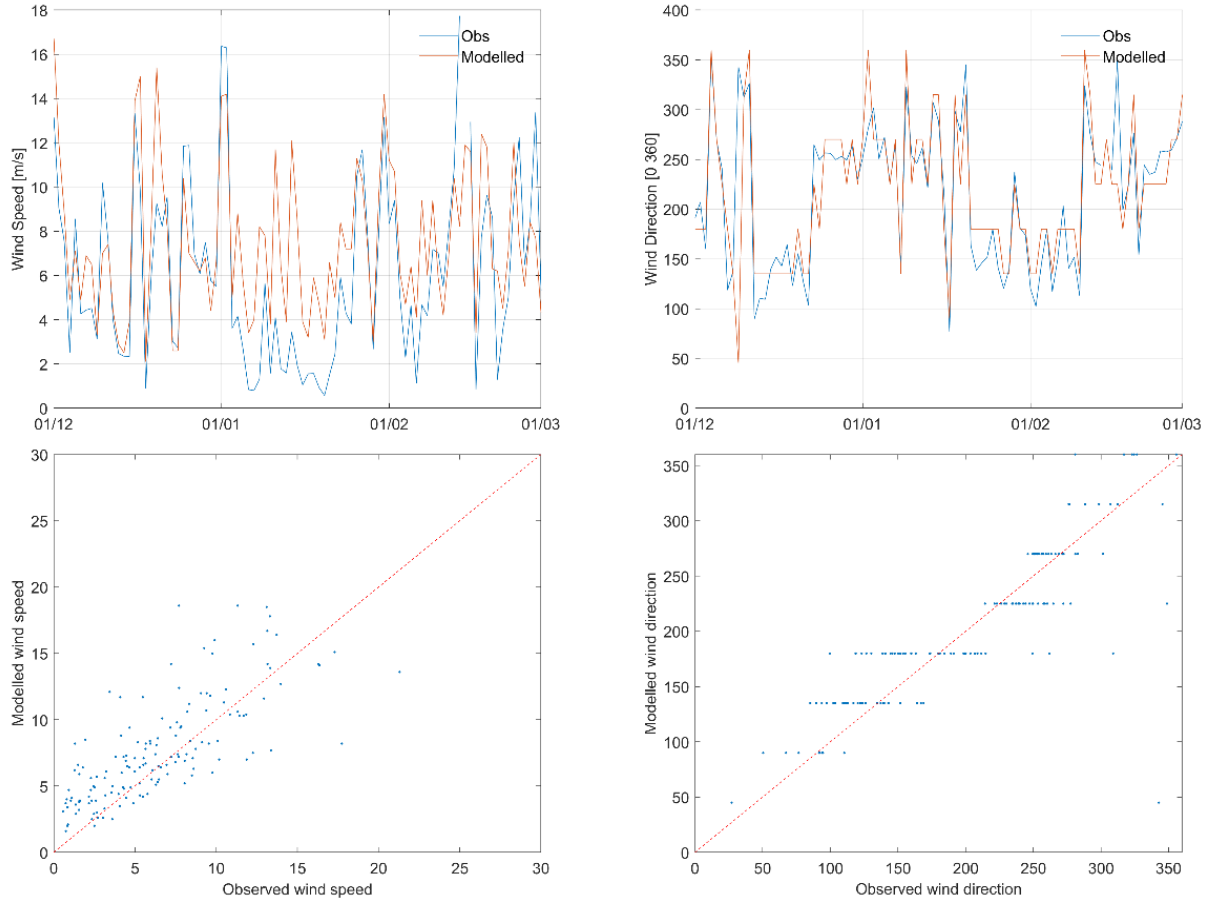

Figure 1: Wind Speed and Direction observed at Kvitenova for the period Dec 2018 - March 2019, compared to data modelled in Arome for the same coordinate.

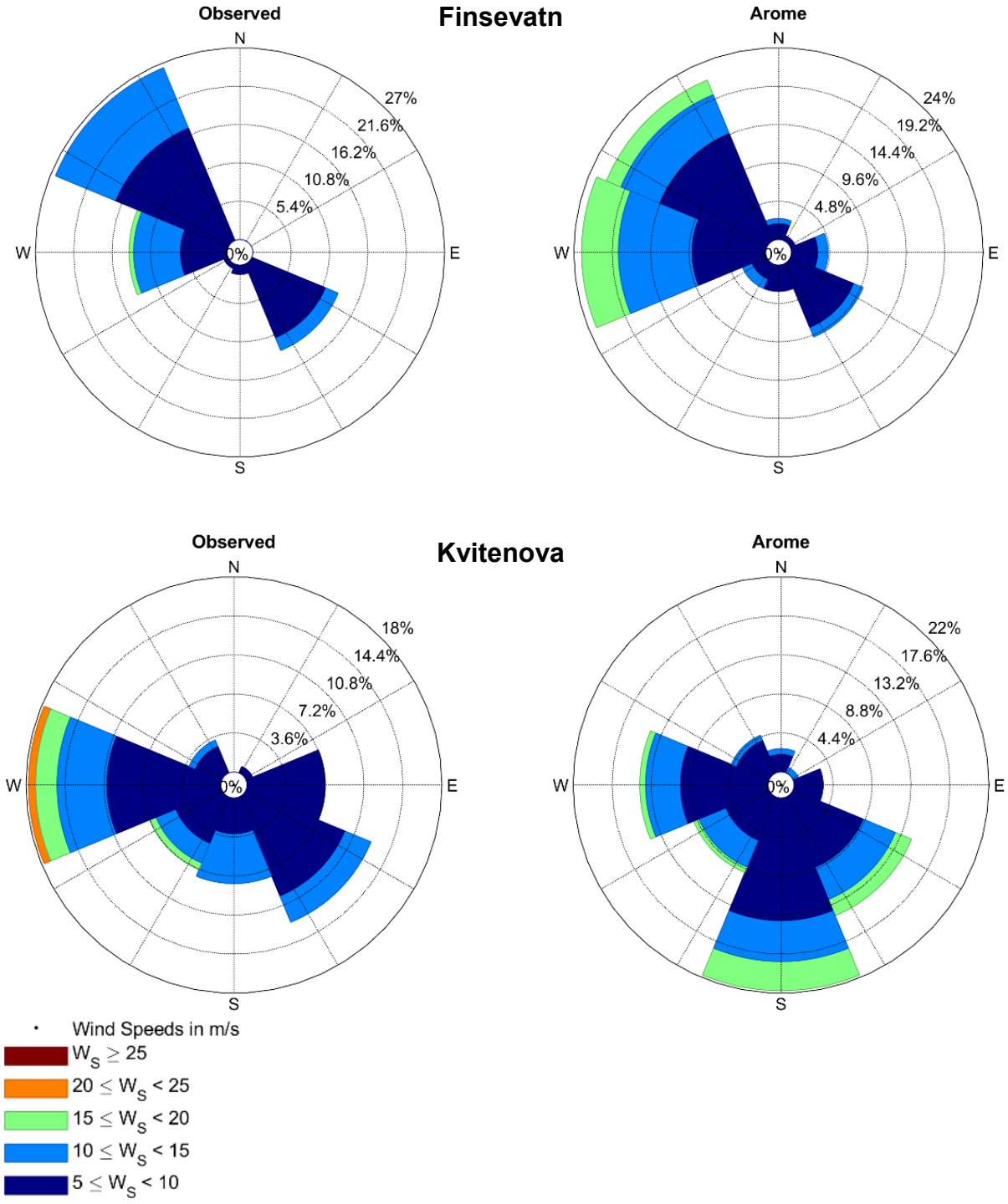

Figure 2: Upper: Observed (left) and modelled with AROME (right) wind distribution for 2018 - 2019 at Finsevatn (upper) and Kvitenova (lower). The wind speed colour scheme is used for all wind roses in this chapter.

3 Wind field simulations with WindSim

Detailed knowledge of wind speed and direction patterns is crucial to understanding the redistribution patterns of snow in mountainous areas. This fine scale wind distribution and lee effects from detailed terrain features is not resolved by regional scale weather models such as AROME. Inclusion of terrain parameters such as the sheltering index described above succeeds to some extent in reproducing leeward areas and is helpful for creating a rough overview of potential release areas. However, the magnitude and detailed position of large snow depositions cannot be reproduced. Significant snow deposition areas relevant for avalanche formation in Norway depends heavily on wind speeds over upstream fetch areas, acceleration/deceleration over ridges, and local wind fields. These effects can only be captured by more sophisticated wind representations.

WindSim is a Norwegian-developed state-of-the-art CFD modelling software built to optimize representation of wind. The software is also widely used for research on air pollution, icing on electricity lines etc., and was found to be the best alternative for testing a commercial CFD wind software package for snow transport. The software is prepared for rather coarse scale resolution terrain models as input and high-altitude wind fields. For our purposes high resolution terrain features are of interest as well as near-surface wind fields. Our use is therefore a new application of the software, and available methods for input data generation and import could not be used. As there are no standard formats for input and output data of neither terrain, roughness nor climate data, but rather specific WindSim formats, an unforeseen amount of resources was used to develop tools to generate terrain data files from GIS, climate data input files and import-routines of vector wind fields to GIS. There were also technical challenges related to software and installation, and in total fewer actual tests than planned have been conducted. However, several model runs are now done, and 8 directional wind maps have been made for several areas. Model examples were presented at Snøskredkonferansen at Voss, 2019. Wind fields produced by WindSim showed useful results for the evaluation of drifting snow challenges at Kvænangsfjellet.

3.1 New WindSim tools

New tools have been developed to produce input files and integrate use of WindSim with GIS-tools. Scripts for validation of transferred timeseries of wind data have also been developed.

1. 1. Tool for export of terrain and roughness data from ArcGISpro including stand-alone python script to convert from ASCII format to. gws-format
2. 2. Script to generate input climatology file in tws-format (timeseries) for selected weather station – MATLAB
3. 3. ArcGISpro tool to import XY vector fields of wind from WindSim and convert these into arrows and continuous wind speed raster.
4. 4. Script to read and validate transferred climatologies to observed data - MATLAB

3.2 Resolution and distribution of cells

WindSim has primarily been run based on the national 10 m DEM from the Norwegian Mapping Authority. However, the initial run must solve for unknown boundary conditions, and the size of the first run has to be large enough to both capture major topographical features and wind fields in the area, and the area of interest should be far from the edges in order to minimize boundary effects. Initial runs are therefore resampled to coarse resolutions of > 50 m in horizontal spacing. In a second model run the wind fields from the first run can be used as boundary conditions, and by utilizing such nesting techniques we can get down to the resolution and altitude levels relevant for snow distribution processes. In this study we have used two nests for all test areas.

The main capacity requirements driver is the maximum number of cells included in the model run. We have run simulations of up to 1 000 000 cells, and this takes 3-4 hours under "normal" server capacity. The number of cells is the total of the 3D grid, and the ground resolution is a function of the decided maximum number of cells, and the number of vertical layers. On one hand, the distribution of nodes in the vertical direction should be as dense as possible to obtain accurate numerical solutions, in particular near the ground. This requirement implies that the upper boundary should be placed as near the ground as possible. Yet, on the other hand, if the upper boundary is too close to the ground this would impose a blocking effect when the flow field passes over mountains. The vertical profile should be high enough that the relative variation in vertical space between the terrain and top of the vertical profile is low. In avalanche terrain the elevation differences are often large, and fulfilling these requirements is challenging.

The sizing of the vertical grid follows an arithmetic sequence, and the factor difference between the size of the uppermost and the lowermost cell can be adjusted. In order to capture the near-surface wind flow as well as the high ground resolution we used a factor down to 0.05, which seemed to give good results.

In nest 1 an area of around 10x10 km was typically chosen, with 20-25 vertical layers and a grid resolution of around 50 meters. In nest 2 a smaller area of about 5x5 km was selected, with 20 vertical layers, a scaling factor of 0.05, and with a refined grid in the center of the model area. It is therefore crucial to center the refined grid around the area of interest. The parameters were set so that the obtained ground resolution was down to 10 meters in the refined grid, and the lowest vertical layer at around 10 meters height above ground.

3.3 The generation of wind fields

Wind fields for selected wind directions are generated in a step 2 when a terrain model and 3D grid is made for the model area. Wind fields were in general made for a uniform distribution of 8 wind directions, while default settings are used for temperature, air density, turbulence models, solvers and convergence settings. In nest 1 speed above the boundary layer must be set. For snow transport speeds above 10 m per second should be

used, and results indicate that higher speeds of 15 m/s are recommended. In nest 2 wind fields from nest 1 are imported as boundary and initial conditions.

After wind fields in nest 2 (or the innermost nest) are generated, the wind fields are exported to vector fields in a step 3 (Results tab). Here, velocity vectors XY at selected heights (ideally down to 10 m above ground but depending on the vertical profile) are exported for all wind directions. This output is thereafter imported to ArcGISpro using the import-tool.

Wind fields are generated for Grasdalen, Strynefjellet, Finse, Tyin, Stryn Valley (for storm surge analysis).

3.4 Validation of transferred climatologies

The ability to generate transferred climatologies for selected points in the model domain is available under the "Objects" tab. This tool is primarily built to estimate wind effect and potential energy production for selected turbine locations. However, we have used this tool to investigate how well the wind field is represented in the terrain, in areas where several wind observations are available within short distances. Hourly time series of wind speed and direction from a reference station, ideally capturing the more large scale wind fields, is used as input to WindSim. Transferred climatologies (i.e. wind speed and wind direction for each time step in the input time series) are generated in locations where timeseries of similar wind data is available. This has been tested for Grasdalen, Strynefjellet and Finse.

3.5 Validation of modelled wind fields in Grasdalen:

Strynefjell_nest2: 33 – 350 m grid spacing in x, y direction, 50 cells in z direction, height distribution factor 0.1, lowermost vertical layer at 9.5 – 12.4 m. Kvitenove is inside, but Fonnbu is just outside the refinement area.

Strynefjell_nest2_Fonnbu2: Grid spacing 22 meters in the fine area where both Kvitenova and Fonnbu is inside the refinement area, the height distribution factor 0.05, and the lowermost vertical layer is at 12.5 – 16.2 m height.

Timeseries of wind data from Kvitenova (UTM33, 98716E, 6896590N, 1400 m a.s.l.) for the period 01/09/2015 - 24/06/2016 was used to transfer climate to Fonnbu (UTM33, 97965.9E, 6898015.5N). The modelled wind data at Fonnbu is compared to observed 10 m wind speed and direction measured at the Fonnbu weather station. Both models have trouble reproducing the complex wind pattern down in the valley where Fonnbu is located (Figure 3). Wind speeds are significantly reduced, too much compared to observations. Main wind direction is not changed much relative to the reference point at Kvitenova, but the shift towards a larger southerly component is partially reproduced. Wind speeds are even more reduced in the Strynefjell_nest2_fonnbu run, where the resolution is finer. The results are not satisfactory, and new model tests adjusting vertical

layers and grid resolution should be performed. However, first of all longer time series of validation data from Fonnbu should be included.

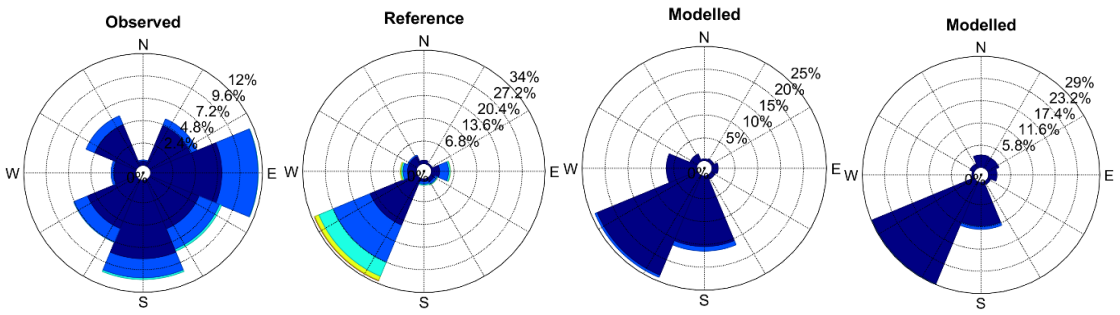

Figure 3: Wind distribution measured (Observed) at Fonnbu research station, the input data set from Kvitenova used for the transferred climatology (Reference), and modelled with WindSim for the location of Fonnbu in the Strynefjell_nest2 (Modelled, left) and Strynefjell_nest2_fonnbu2 (Modelled, right). Color grading refers to wind speeds according to Figure 2.

3.6 Validation of modelled wind fields at Finse

At Finse 10 m wind speed and direction, measured at the official weather station Finsevatn, is used as reference dataset (Figure 4). Just west of Vesle Hansbunut, 1-2 km southwest of the official weather station, a 1 $km2$ study site has been established by the University of Oslo. The area rises around 100 m above the surrounding terrain and features a rough and undulating topography. Three 2 -3 m high temporary weather stations were installed in the fall 2011 (Gisnås et al., in prep, Table 1). The three stations are placed in various exposures in the field area in order to capture the variation in wind pattern. The main wind direction is from northwest, while southeasterly winds are also common. Station A is located in a north-west moderate slope of little curvature facing the prevailing westerly winds. Station B is located in a south-east slope in a positive curvature on the lee side of a hill. Station C is placed near an exposed top just to the east of the study area. This variation in location intends to capture the local topographic effects on wind speed. Precise locations, elevations and sensor heights for each station is found in Table 1. A high resolution snow distribution map (20 cm ground resolution) is avilable for the area, obtained from UAV based SfM photogrammetry by subtracting the summer surface (Sept 2015) from the winter surface at snow maximum (May 2016) (Gisnås et al., in prep; Figure 12).

Table 1: Location of weather stations at Finse given in UTM33 coordinates.

Station	UTM33 Easting	UTM33 Northing	Elevation
25830 Finsevatn	91086.9	6740617.4	1210
Station A	91686.2	6739107.0	1294
Station B	92044.2	6738726.5	1303
Station C	92331.2	6738627.5	1336

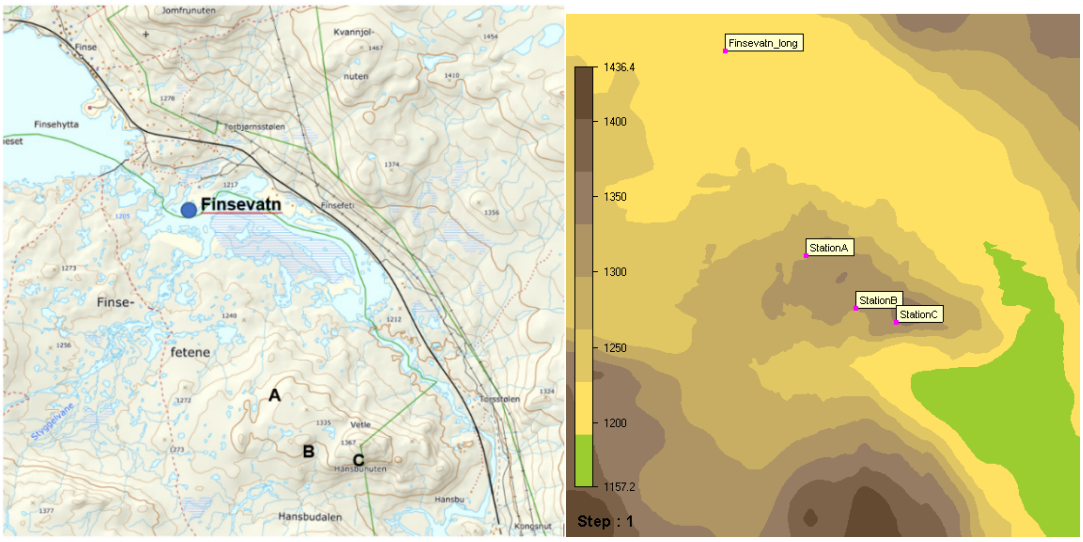

Figure 4: The test area southeast of Finse, with temporary wind stations at location A, B, and C. Right: terrain model used in the model runs.

Transferred timeseries of wind direction and speed were modelled for the stations A, B and C for the period 22nd Oct 2012 – 31st March 2016, based hourly observations of wind speed and direction at 25830 Finsevatn. For all model runs the three validation stations are inside the refinement area, while the Finsevatn reference station is outside. Results from two model runs, Finse_nest2 and Finse_nest2_fine is presented. The stations have different data coverage within the modelled time period. For the comparison at each of the stations, only data available both in the modelled and observed time series is included.

Finse_nest2: Grid spacing of 11.3 meters in the refined grid, and the lowest vertical layer is 4.6 – 5.3 m above ground. The run has 20 vertical layer with a height distribution factor of 0.05.

Finse_nest2_fine: Grid spacing in x and y direction is 10.2 meters in the refinement area and 117 meters outside. 20 vertical layers is distributed with a height distribution factor of 0.03, resulting in the lowest vertical layer beeing 2.9 – 3.3 m above ground.

At Station A the model reproduces the shift from westerly to north westerly main wind direction, and also succeeds in modelling the lee effect from easterly winds. This effect

is slightly improved in the Finse_nest2_fine model run, with higher ground resolution and lowest wind field closer to the ground (Figure 6 and Figure 7). However, wind speeds from west are too high, which may be because the model does not capture the small-scale topography around the station.

At station B the Finse_nest2 model run does not succeed in reproducing the shift towards northwest – south main wind directions (Figure 8). It captures the lee-effect at the site, however, the wind directions and also the higher lee effect from west relative to south is much better reproduced in Finse_nest2_fine (Figure 8, Figure 9 and Figure 10). The modelling at station B demonstrates that there is a significant gain in using near surface winds and high-resolution terrain models for terrain varying within 50 – 100 m in elevation difference.

At station C the modelled wind speeds and directions are very similar for the two model runs. The model suceeds in capturing the change in westerly wind direction towards north west at the station, and also the relative higher wind speeds due to the wind acceleration around the mountain top (Figure 11). However, wind speeds are in general overexaggerated, particularly when coming from the southwesterly direction. Also, the observed shift in wind direction towards south for southeasterly winds is not reproduced. This is probably due to the size of the large terrain model in nesting 1, which does not capture the large scale topography, most notably lacking Hardangerjøkulen to the south.

Station A:

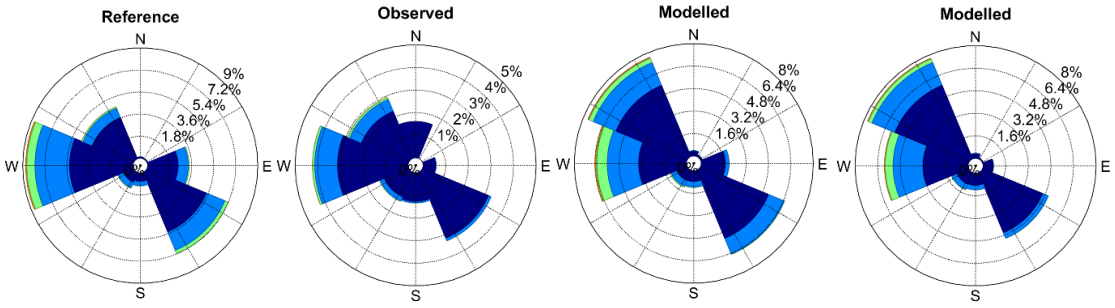

Figure 5: Wind roses for the reference station Finsevatn, the observed wind at Station A, and modelled wind with Finse_nest2 (left) and Finse_nest2_fine (right). See color legend in Figure 2. Wind speeds below 5 m/s are excluded.

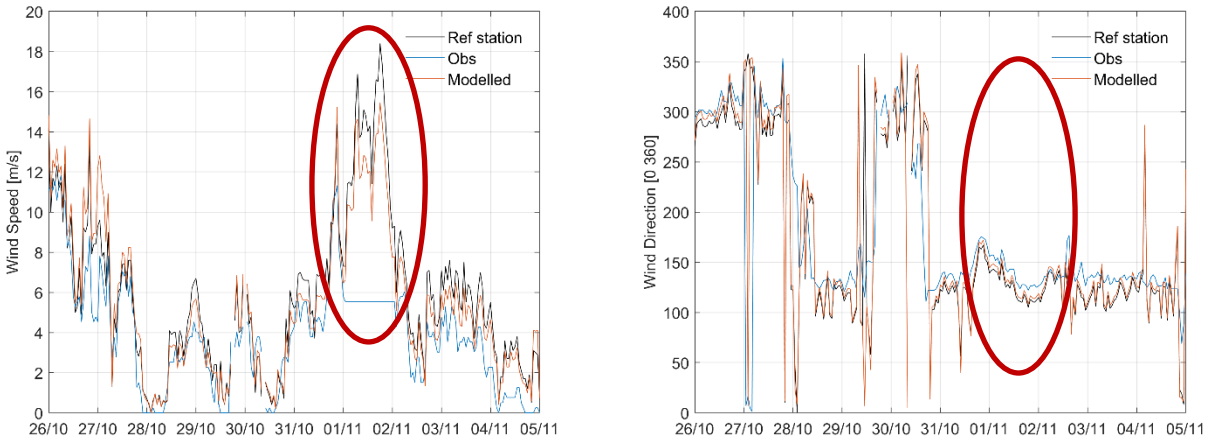

*Figure 6: Reference, observed and modelled wind speed (left) and direction (right) at Station A with the **Finse_nest2** model run.*

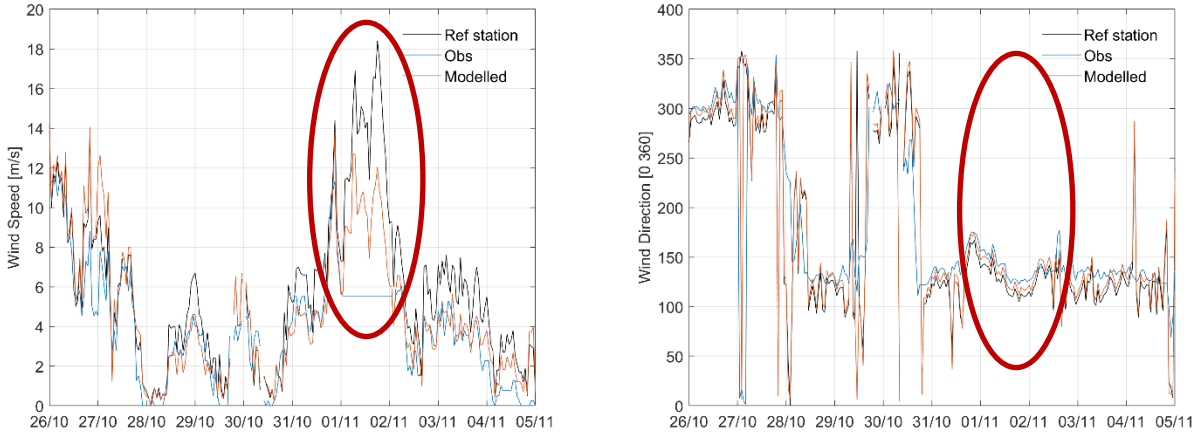

*Figure 7: Reference, observed and modelled wind speed (left) and direction (right) at Station A with the **Finse_nest2_fine** model run.*

Station B:

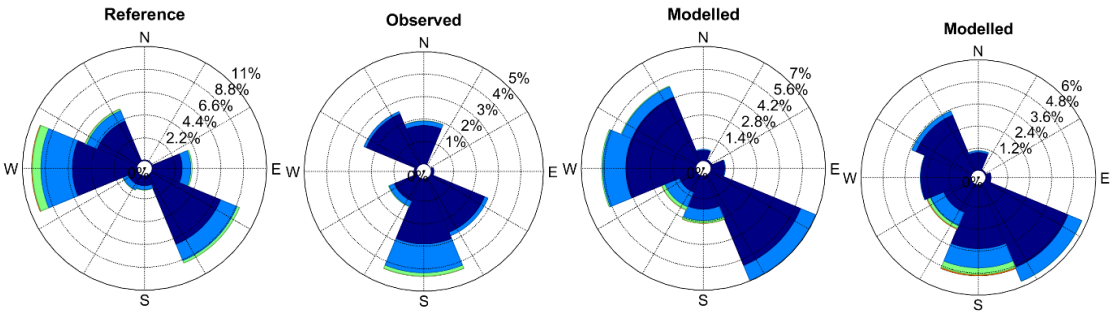

Figure 8: Wind roses for the reference station Finsevatn, the observed wind at Station B, and modelled wind with Finse_nest2 (left) and Finse_nest2_fine (right). See color legend in Figure 2. Wind speeds below 5 m/s are excluded.

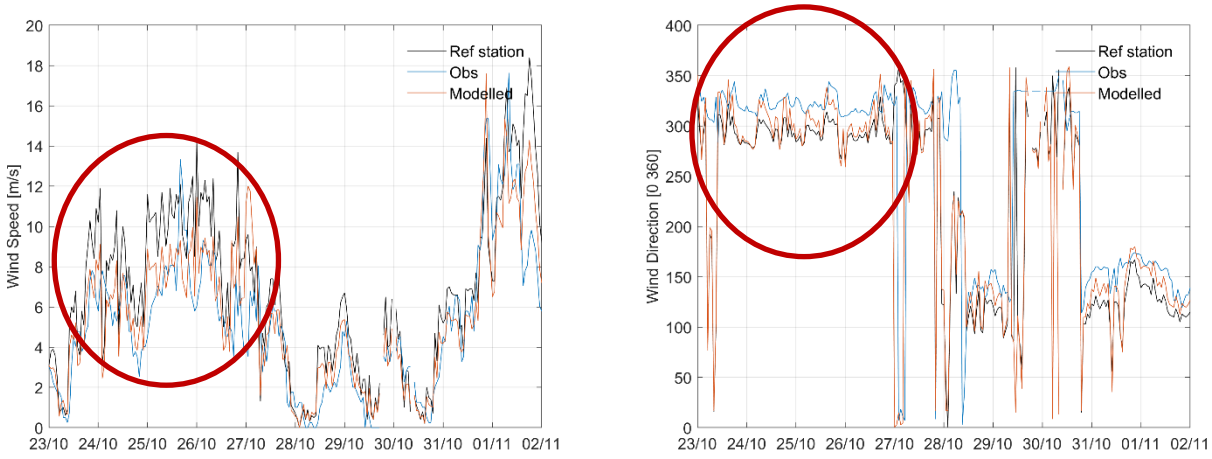

*Figure 9: Reference, observed and modelled wind speed (left) and direction (right) at Station B with the **Finse_nest2** model run.*

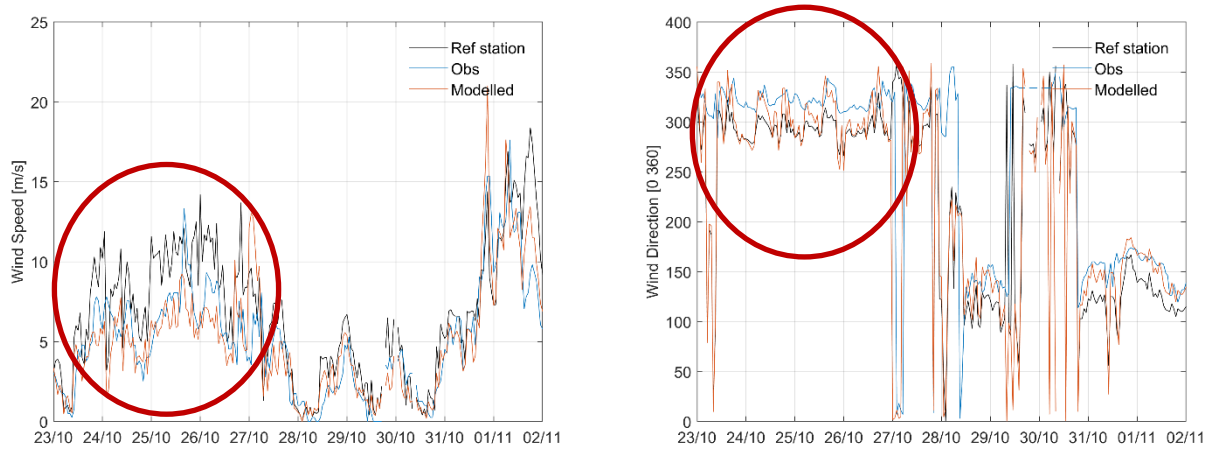

*Figure 10: Reference, observed and modelled wind speed (left) and direction (right) at Station B with the **Finse_nest2_fine** model run.*

Station C:

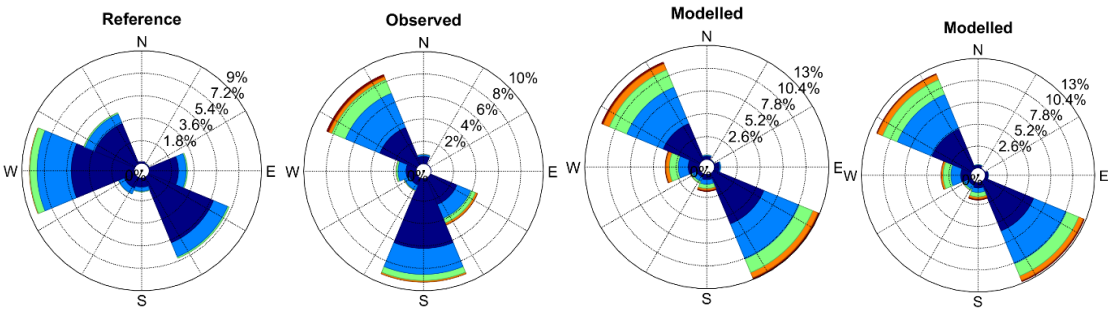

Figure 11: Wind roses for the reference station Finsevatn, the observed wind at Station C, and modelled wind with Finse_nest2 and Finse_nest2_fine. See color legend in Figure 2. Wind speeds below 5 m/s are excluded.

3.7 The use of advanced CFD wind models to determine snow redistribution

At Finse a high-resolution snow height model, provided by UiO, was made at snow maximum in May 2016, based on Structure-for-motion photogrammetry from UAV (Figure 12). Within the 1x1 km test area snow heights varied from 0 to almost 9 meters. This demonstrates the need to represent the snow distribution at a finer scale than the SeNorge snow height grid when studying potential release areas for snow avalanches. Main wind direction during the snow accumulation season 2016 at Finsevatn was westerly, and the snow distribution data is therefore here compared to the vector fields for wind direction 270° in Finse_nest_fine.

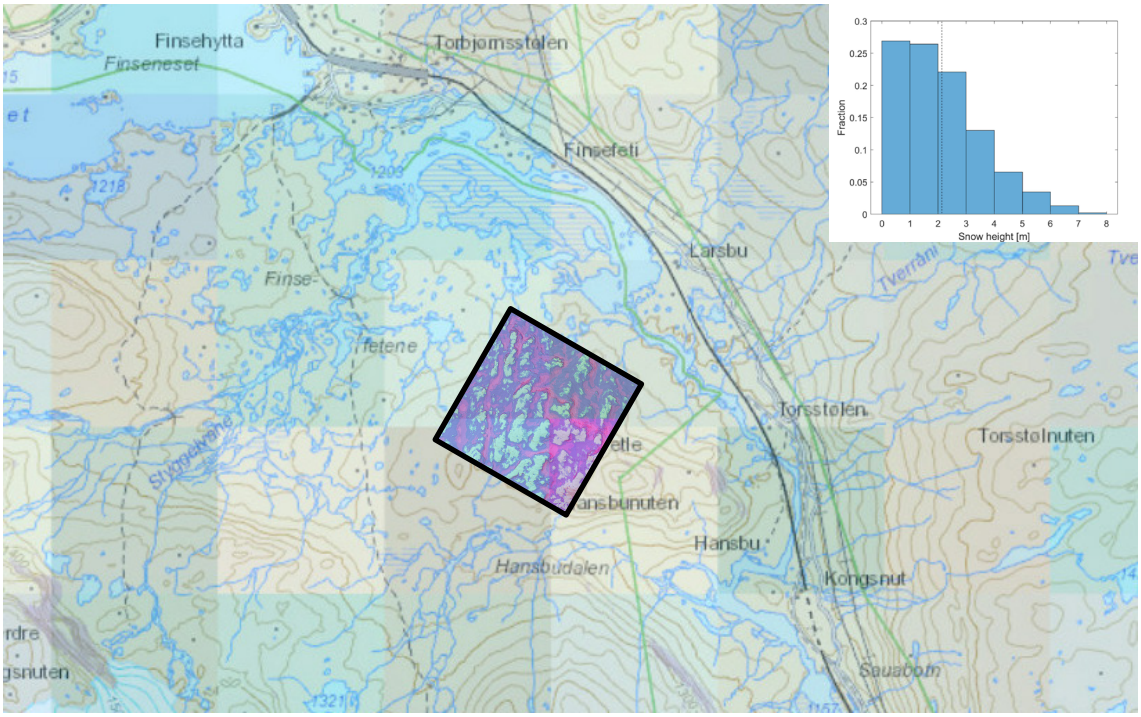

Figure 12: Map showing size of 1 km grid cells at Finse in the background, with the high resolution snow distribution at Vetle Hansbunuten on top (small square). The measured snow distribution within the square is given in upper right corner, showing snow heights of 0 - 9 meters (Gisnås et al., in prep).

The vector field (Figure 13) shows that the undulating topography in general has minor effects on the modelled vector direction. However, in the steepest areas there are some variation in speed and direction. Next to Station B (indicated with a red circle), the wind is accelerating (purple arrow color) over the ridge and decelerates (blue arrow color) on the leeward side. Deep snow accumulation is measured in the location of the strongest deceleration (Figure 13). Also, along a north – south ridge in the west part of map the same effect in the vector field coincides with a deep snow accumulation (red elongated circle). The two sites of heavy snow accumulation can also be identified from the

continuous velocity map (Figure 14), as areas with strong gradient from high to low velocity. The snow free areas are only to some degree coinciding with the areas of highest wind speed (Figure 13).

The model runs show promising results for determining potential areas of great snow deposition, however, the requirements to model resolution is very high in order to capture lee effects from terrain variations of only 20 – 30 meters, which is the case at the two highlighted areas in Figure 13 at Finse. In case of terrain variations below this, several nests should be used to achieve a high enough resolution.

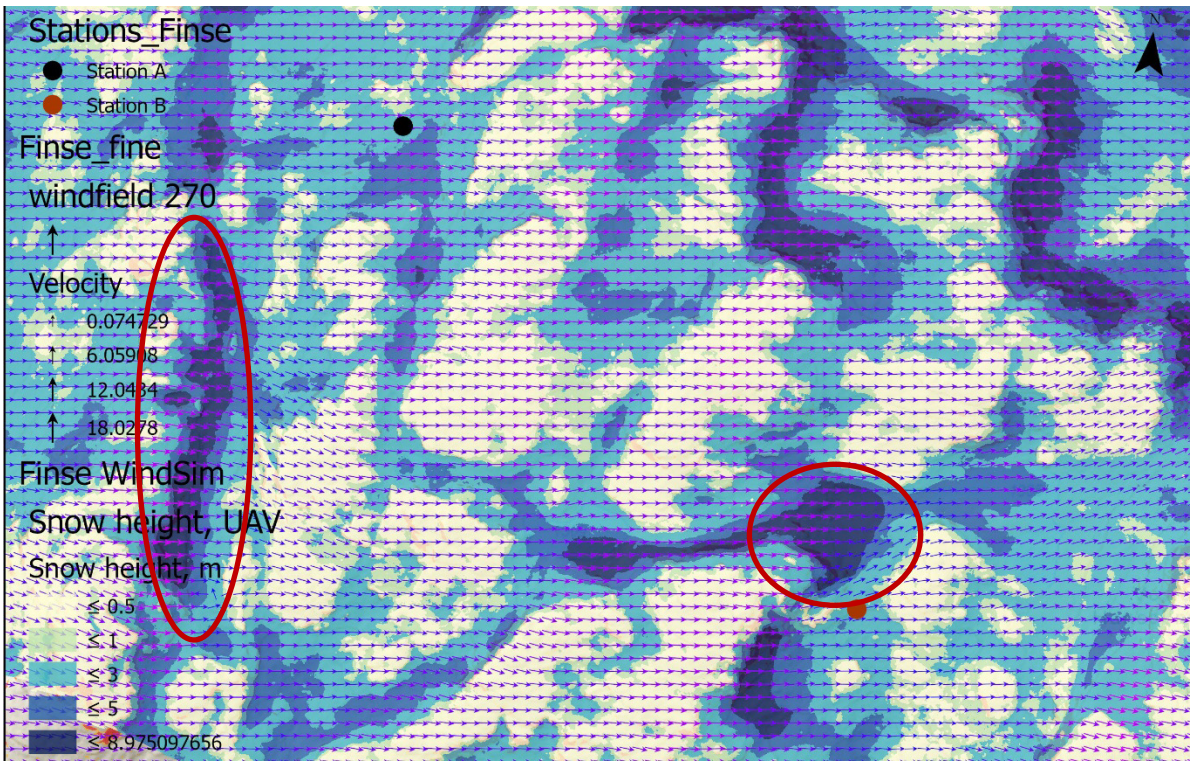

Figure 13: Vector field for main wind direction 270° over observed snow distribution May 2016 from UAV. Distance between the two stations are approximately 450 m.

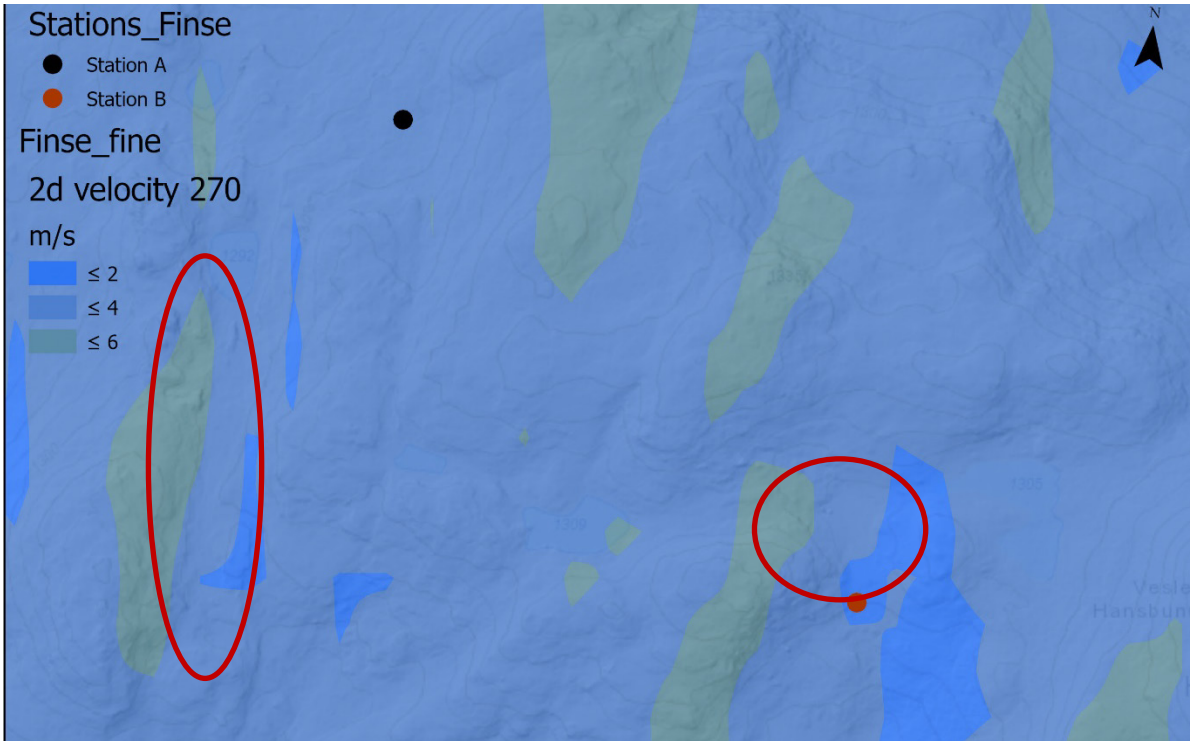

Figure 14: Velocity field for wind direction 270° modelled in the run Finse_nest2_fine. Red circles indicated locations of strong deceleration and snow accumulation indicated in Figure 13.

3.8 The use of terrain indexes and advanced CFD wind models to determine potential release areas

The Winstral sheltering index provides a quick overview of lee areas for a given wind direction. At Sæterskarsfjellet in Grasdalen avalanches are often released after precipitation and westerly to north westerly winds. The SX-factor for 8 wind directions is derived from the same 10m resolution DEM as used for the WindSim runs, and here shown for values above 0.6 (orange) and 0.7 (red). For westerly winds (270°) the highlighted potential release areas fits well the major observed release areas (Figure 15). For northwesterly winds, only release areas in the southern side of Sæterskarsfjellet are highlighted, even though we know that northwesterly winds can result in avalanches also along the ridge. Due to terrain effects on the wind field, wind may still come from westerly directions when the main wind direction is north westerly. To account for these effects, we therefore need physical representation of the wind field. Correctly, the same index does not reveal any potential release areas in the test area at Finse.

The vector field from west (270°) modelled in Strynefjell_nest2_fonnbu2 shows that westerly winds tend to approach the lower part of the ridge from south-westerly direction. As the valley side to the southwest is very steep, there is limited snow available for transport. In the upper part significant accumulation would be expected as the wind decelerates as it crosses the edge down from the plateau. From this model

simulation it may look like the strongest deceleration happens somewhat down and northeast of the uppermost release areas, however, this should be further investigated with more detailed model runs.

In the vector field for winds from northwest (315°) the wind tends to approach the ridge from a north to north-westerly direction, with strong deceleration along the entire ridge (Figure 17). The fetch area from this direction is large, with flat to more gentle slopes to the north and northwest of the ridge. This situation is likely to result in releases from the release areas on the edge of the ridge.

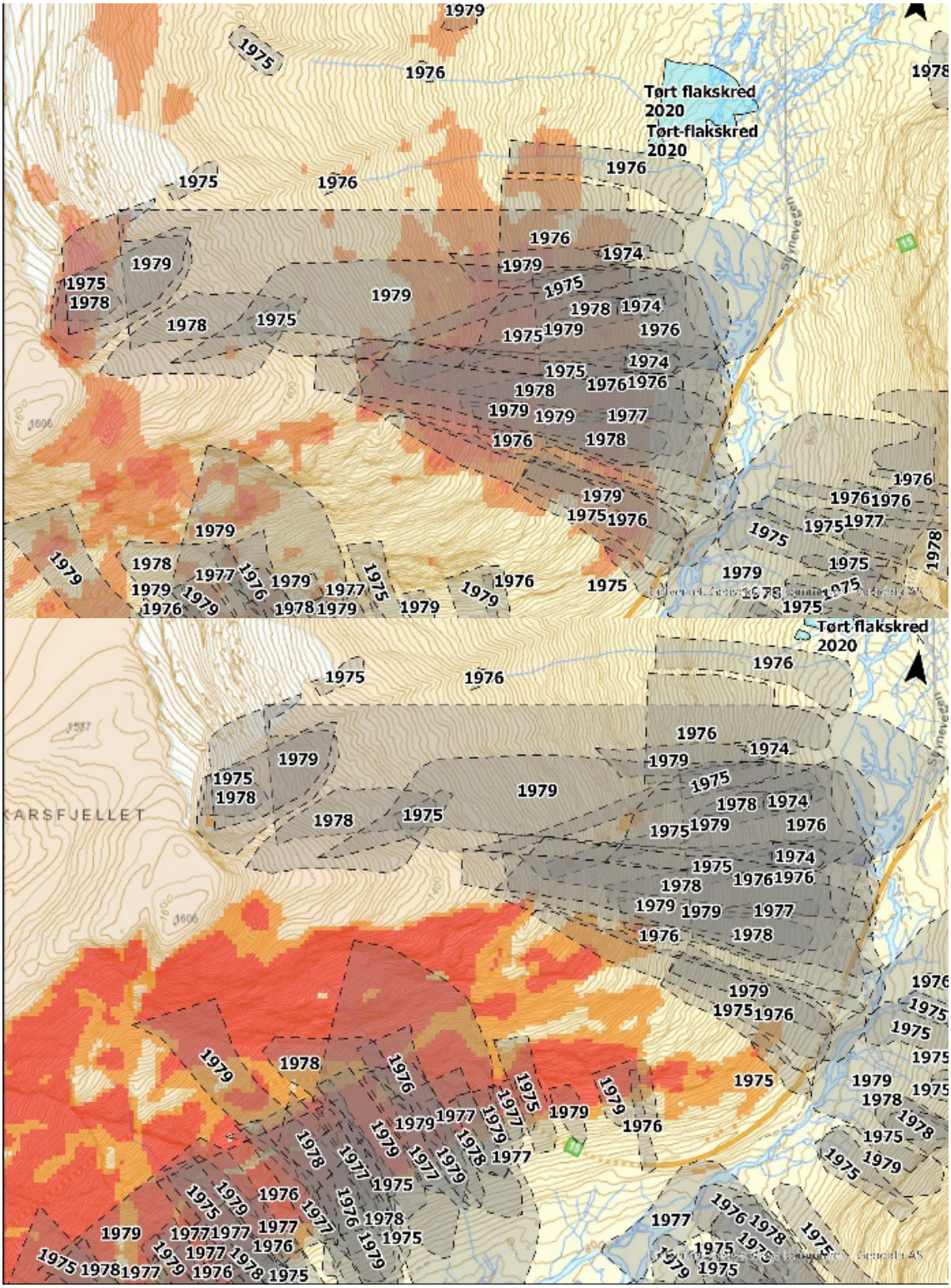

Figure 15: Winstral sheltering index for values above 0.6 (orange) and 0.7 (red) for wind direction from 270° (upper) and 315° (lower) at Sætreskarsfjellet. Observed avalcnhe paths are shown on top.

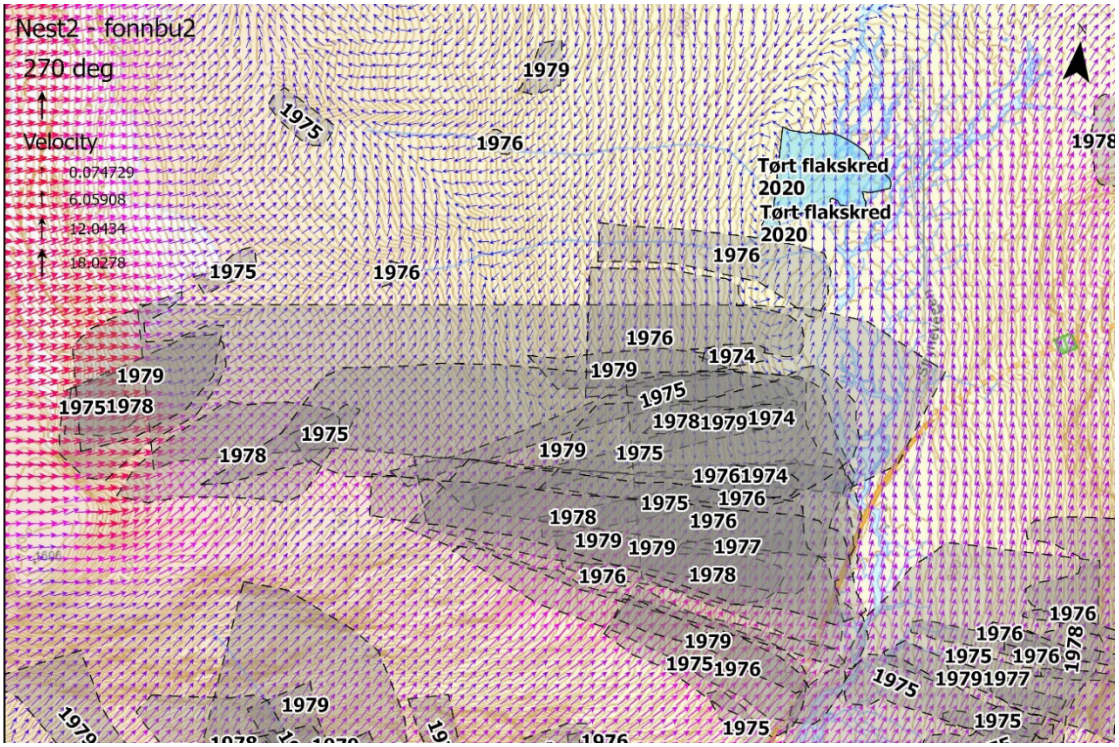

Figure 16: Vector field for wind from 270° at Sæterskarsfjellet exported from the Strynefjell_nest2_fonnbu2 model run. Observed avalanche paths are shown as grey polygons.

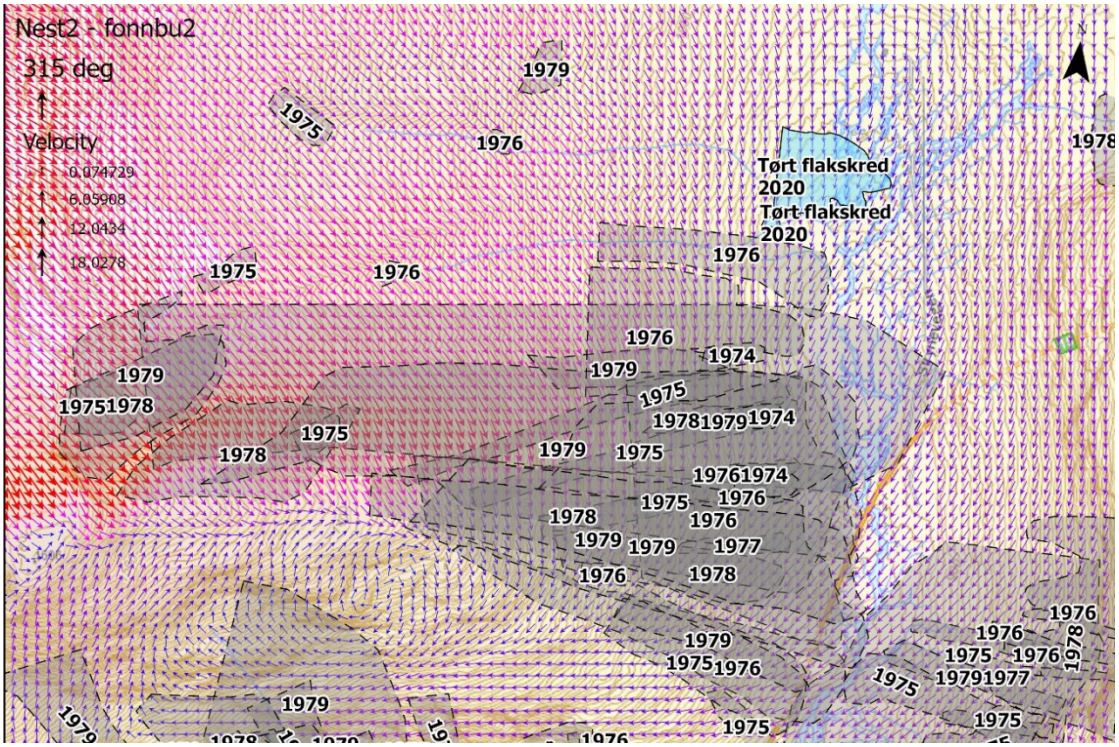

Figure 17: Vector field for wind from 315° at Sæterskarsfjellet exported from the Strynefjell_nest2_fonnbu2 model run. Observed avalanche paths are shown as grey polygons.

In the continuous velocity map (Figure 18) we find a low speed area in the middle part of the ridge at Sætreskarsfjellet. However, without knowing the exact wind direction over the ridge at this point, it is difficult to understand the snow deposition pattern.

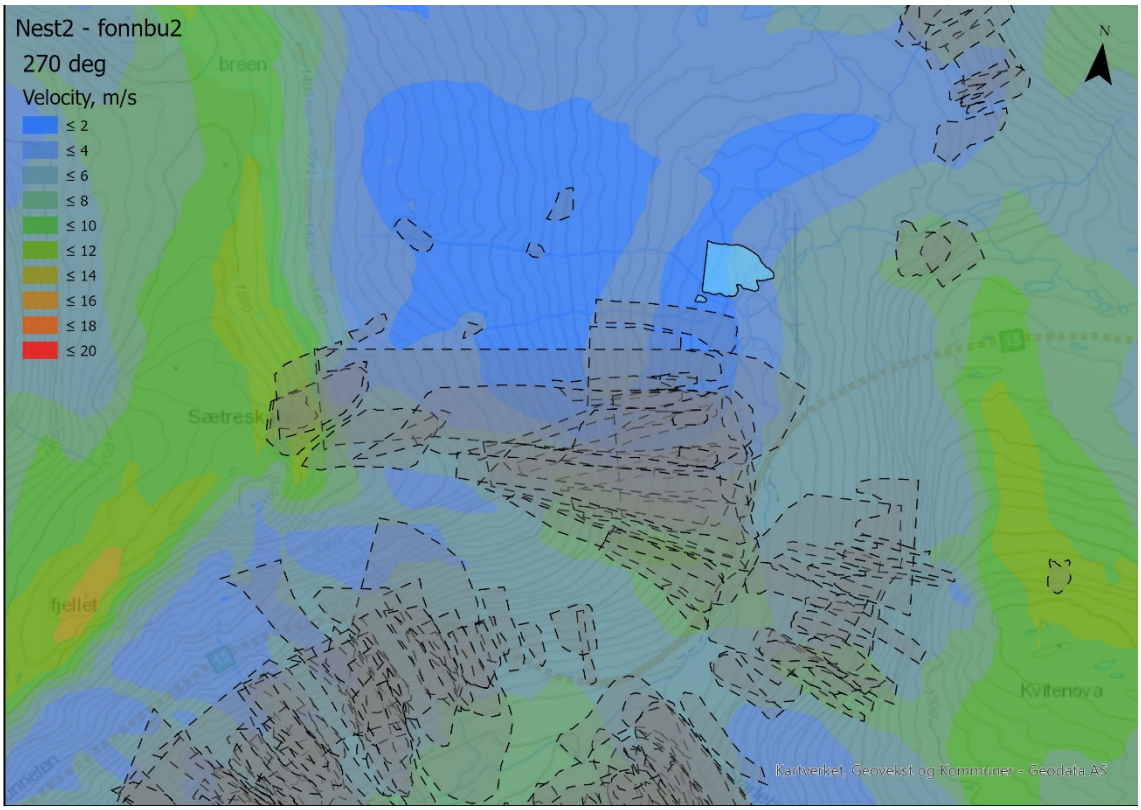

Figure 18: Velocity map for winds from 270° at Strynefjellet. Avalanche paths are shown as grey shaded polygons.

4 Conclusions

The results from the WindSim modelling at Strynefjellet shows great potential for understanding snow deposition and distribution of potential release areas in connection to major wind directions in complex terrain. Detailed analysis are required to make use of the data, and for more quick overviews a terrain index model will provide useful information for very little cost. However, to understand complex deposition patterns, and to track release probability in a specific potential release area to prevailing wind directions, physical models with at a complexity level of the WindSim model is very useful.

To further develop the method and suitability of CFD wind modelling for snow avalanche forecasting, a function to produce continuous raster's of acceleration and deceleration areas from vector fields should be developed. The effect of terrain

resolution and vertical layers in the model setup should also be further explored. Information of snow accumulation in release areas in relation to specific storms would highly benefit validation of future studies.

5 References

Gisnås K., Filhol S., Schuler T.V. (in prep). Distributed meteorological, snow depth, and snow stratigraphy data at Finse, Norway, 2012-2016.

Appendix

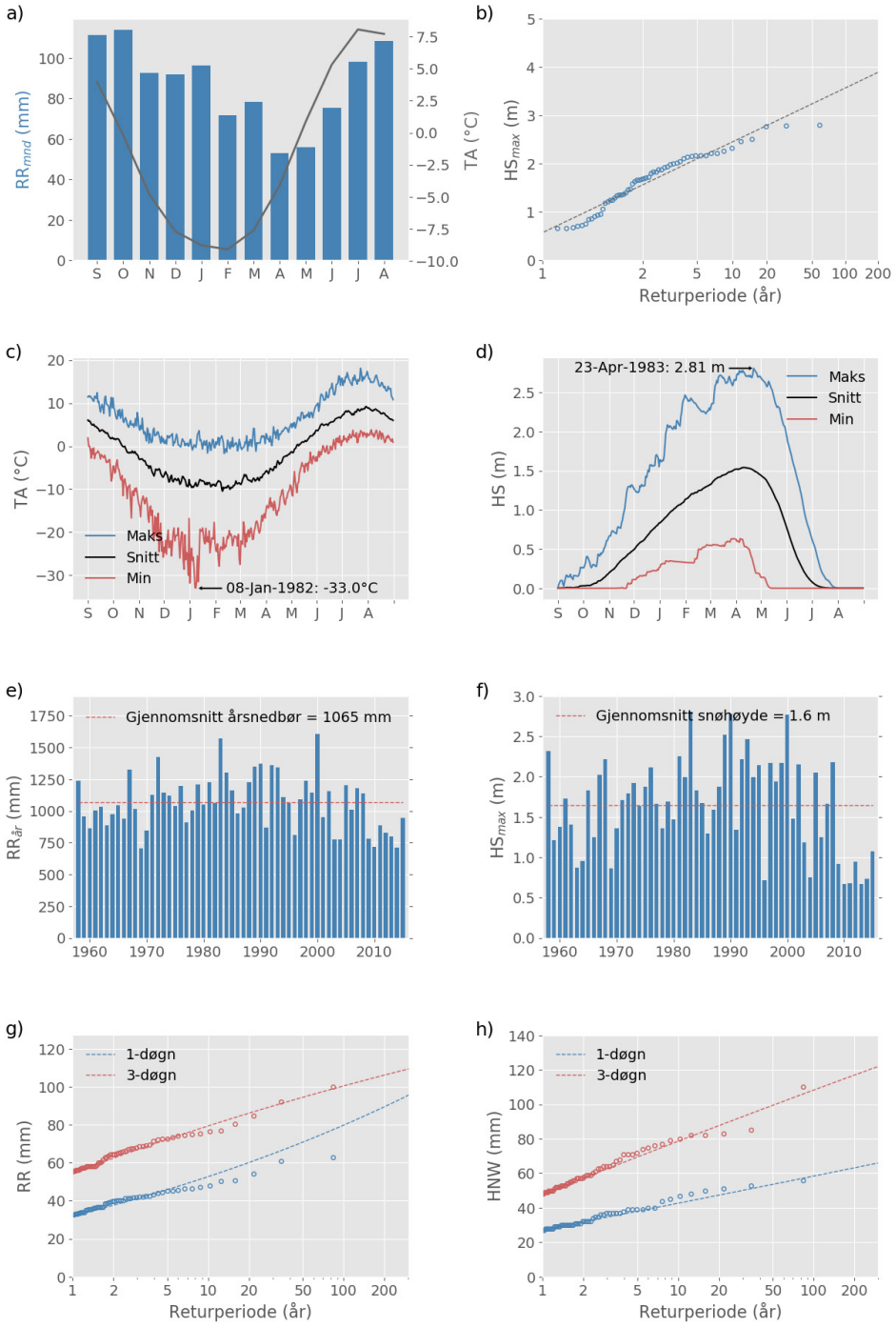

Figure 19: Climate profile for Fonnbu research station at Strynefjellet based on historical SeNorge data (1957 – 2019). a) Monthly precipitation (RR) and temperature (TA), b) return values (gumbel) of annual maximum snow height (HS). Daily min, max, and mean temperature (c) and snow heights (d). Time series of annual precipitation (e) and snow height (f). Return values (peak-over-threshold) for 1- and 3- day precipitation (g) and snow accumulation (h).

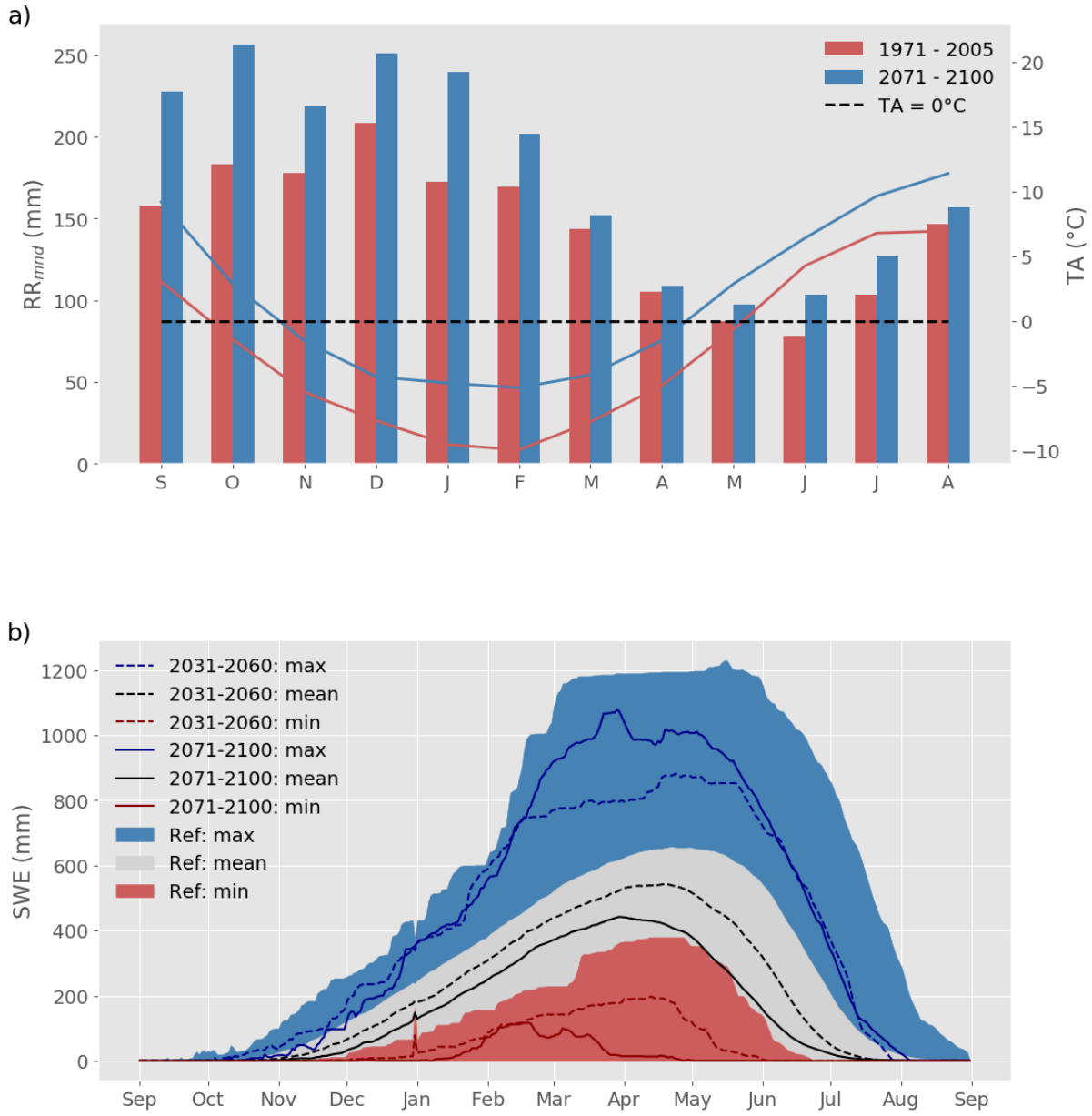

Figure 20: Predicted future changes in precipitation, temperature (upper) and snow water equivalent (lower) at Finse, based on the climate predictions model and scenario IPSL-rcp8.5 downscaled for Norway by the National Climate Services.

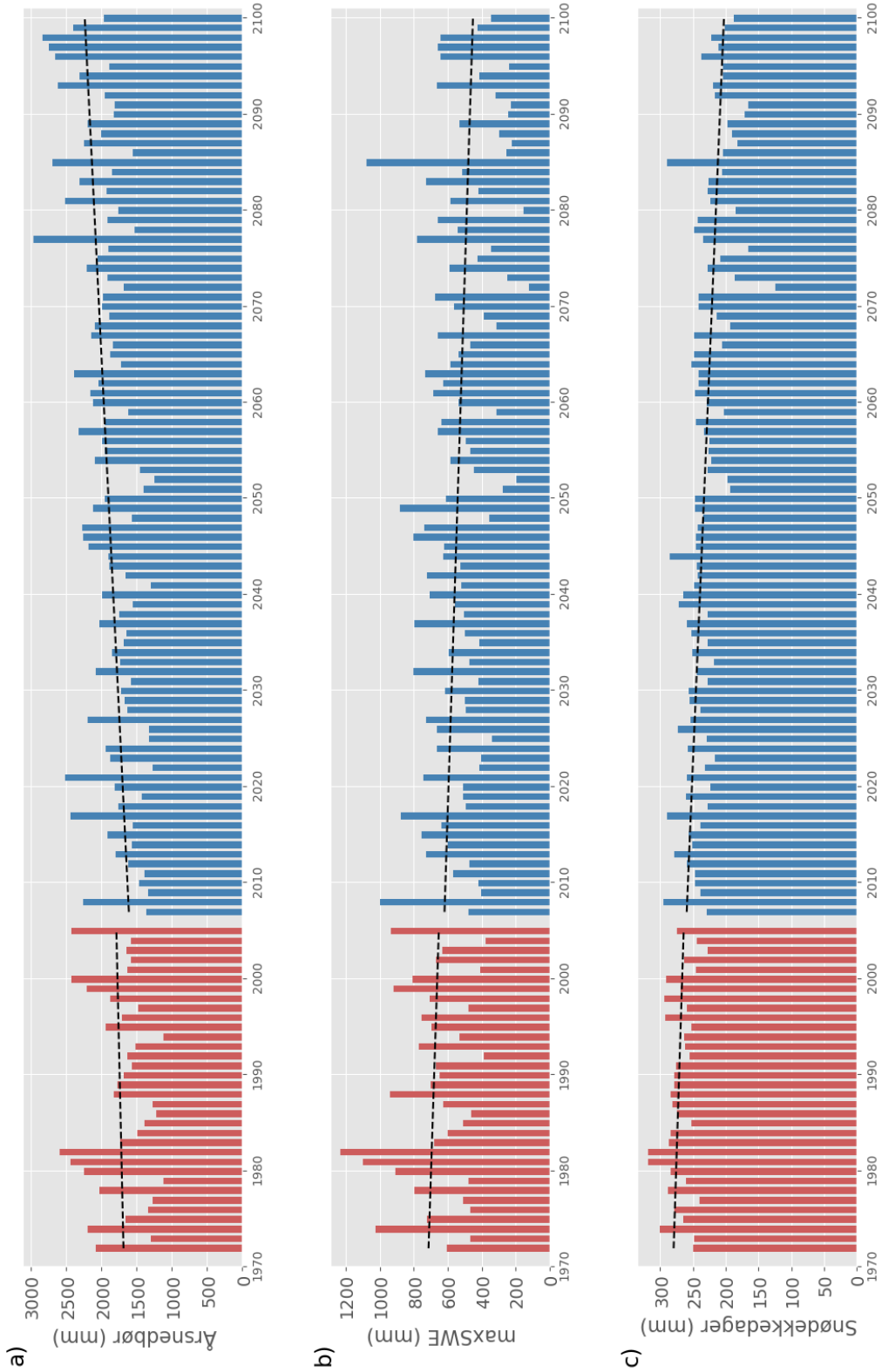

Figure 21: Predicted changes in annual values for precipitation (a), maximum snow water equivalent (b) and snow-covered days (swe > 5 mm) (c) Days with snow cover > 5 cm.

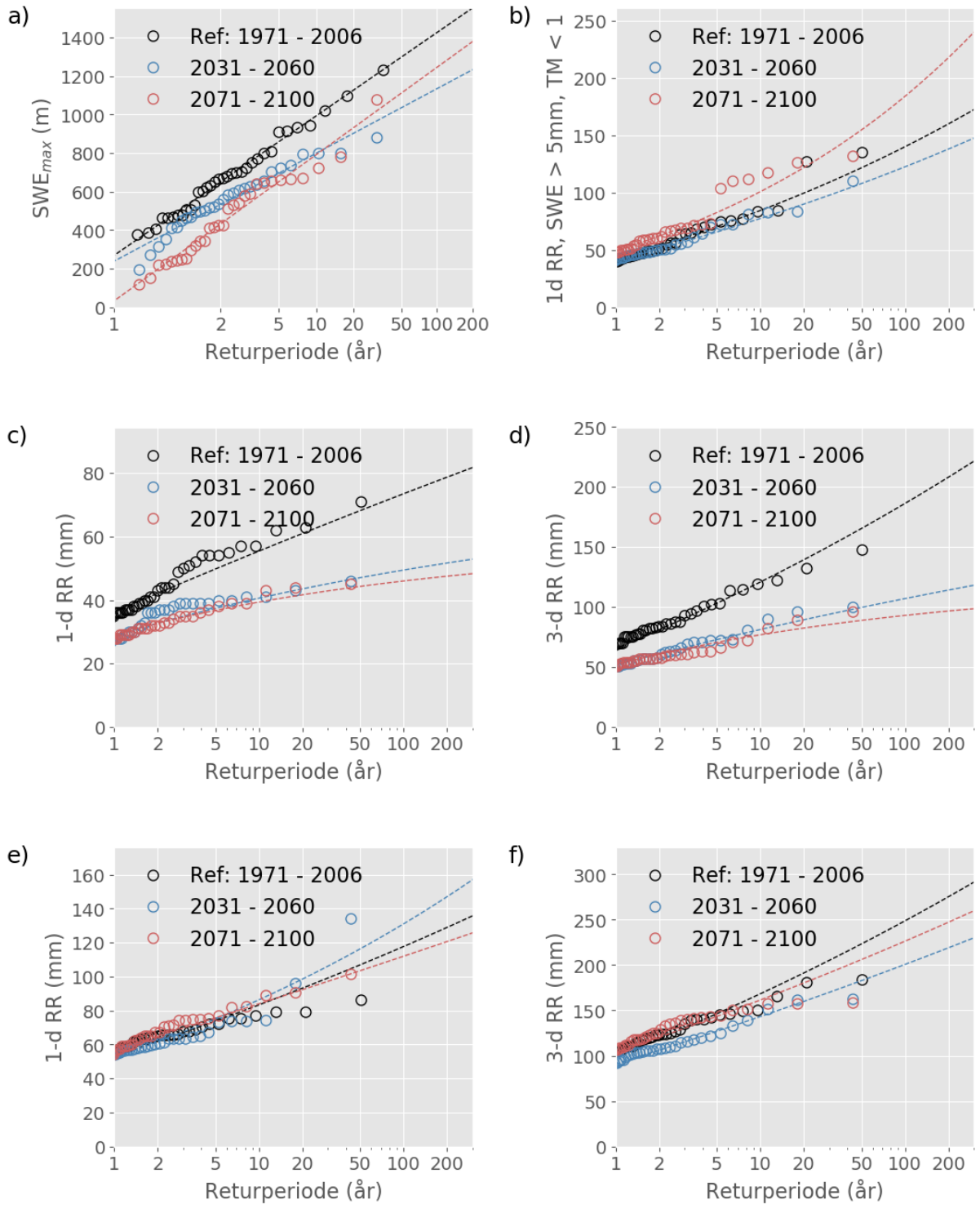

Figure 22: Extreme value statistics showing relative changes in frequency of extreme events of relevant precipitation variables from the reference period to future climates, based on climate prediction model and scenario IPSL-rcp8.5. Location: Finse.

Kontroll- og referanseside/ Review and reference page

Dokumentinformasjon/*Document information*		
Dokumenttittel/*Document title* Vindsimuleringer med WindSim for snøfordeling		**Dokumentnr./*Document no.*** 20170131-19-TN
Dokumenttype/*Type of document* Teknisk notat / Technical note	**Oppdragsgiver/*Client*** Norges vassdrags- og energidirektorat (NVE)	**Dato/*Date*** 2020-06-26
Rettigheter til dokumentet iht kontrakt/ *Proprietary rights to the document according to contract* NGI		**Rev.nr.&dato/*Rev.no.&date*** 0 /
Distribusjon/*Distribution* FRI: Kan distribueres av Dokumentsenteret ved henvendelser / FREE: Can be distributed by the Document Centre on request		
Emneord/*Keywords* Wind simulation, snow distribution, Windsim, Winstral		

Stedfesting/*Geographical information*	
Land, fylke/*Country*	**Havområde/*Offshore area***
Kommune/*Municipality*	**Feltnavn/*Field name***
Sted/*Location*	**Sted/*Location***
Kartblad/*Map*	**Felt, blokknr./*Field, Block No.***
UTM-koordinater/*UTM-coordinates* **Zone: East: North:**	**Koordinater/*Coordinates*** **Projection, datum: East: North:**

Dokumentkontroll/*Document control*
Kvalitetssikring i henhold til/*Quality assurance according to NS-EN ISO9001*

Rev/ *Rev.*	**Revisjonsgrunnlag/*Reason for revision***	**Egenkontroll av/ *Self review by:***	**Sidemanns-kontroll av/ *Colleague review by:***	**Uavhengig kontroll av/ *Independent review by*:**	**Tverrfaglig kontroll av/ *Interdisciplinary review by:***
0	Original document	2020-05-12 Kjersti Gisnås	2020-06-24 Christian Jaedicke		

Dokument godkjent for utsendelse/ *Document approved for release*	**Dato/*Date***	**Prosjektleder/*Project Manager***
	26 June 2020	Christian Jaedicke

NGI (Norwegian Geotechnical Institute) is a leading international centre for research and consulting within the geosciences. NGI develops optimum solutions for society and offers expertise on the behaviour of soil, rock and snow and their interaction with the natural and built environment.

NGI works within the following sectors: Offshore energy – Building, Construction and Transportation – Natural Hazards – Environmental Engineering.

NGI is a private foundation with office and laboratories in Oslo, a branch office in Trondheim and daughter companies in Houston, Texas, USA and in Perth, Western Australia

www.ngi.no

NGI (Norges Geotekniske Institutt) er et internasjonalt ledende senter for forskning og rådgivning innen ingeniørrelaterte geofag. Vi tilbyr ekspertise om jord, berg og snø og deres påvirkning på miljøet, konstruksjoner og anlegg, og hvordan jord og berg kan benyttes som byggegrunn og byggemateriale.

Vi arbeider i følgende markeder: Offshore energi – Bygg, anlegg og samferdsel – Naturfare – Miljøteknologi.

NGI er en privat næringsdrivende stiftelse med kontor og laboratorier i Oslo, avdelingskontor i Trondheim og datterselskaper i Houston, Texas, USA og i Perth, Western Australia.

www.ngi.no

OSLO
TRONDHEIM
HOUSTON
PERTH

NORWEGIAN GEOTECHNICAL INSTITUTE
NGI.NO

Main office
PO Box 3930 Ullevaal St.
NO-0806 Oslo
Norway

Trondheim office
PO Box 5687 Torgarden
NO-7485 Trondheim
Norway

T (+47)22 02 30 00
F (+47)22 23 04 48
NGI@ngi.no

BIC NO. DNBANOKK
IBAN NO26 5096 0501 281
ORGANISATION NO.
958 254 318MVA